

Review

Performance-Driven Yield Optimization of High-Frequency Structures by Kriging Surrogates

Sławomir Koziel ^{1,2}  and Anna Pietrenko-Dabrowska ^{2,*} ¹ Engineering Optimization & Modeling Center, Reykjavik University, 102 Reykjavik, Iceland; koziel@ru.is² Faculty of Electronics, Telecommunications and Informatics, Gdansk University of Technology, 80-233 Gdansk, Poland

* Correspondence: anna.dabrowska@pg.edu.pl

Abstract: Uncertainty quantification is an important aspect of engineering design, as manufacturing tolerances may affect the characteristics of the structure. Therefore, the quantification of these effects is indispensable for an adequate assessment of design quality. Toward this end, statistical analysis is performed, for reliability reasons, using full-wave electromagnetic (EM) simulations. Still, the computational expenditures associated with EM-driven statistical analysis often turn out to be unendurable. Recently, a performance-driven modeling technique has been proposed that may be employed for uncertainty quantification purposes and can enable circumventing the aforementioned difficulties. Capitalizing on this idea, this paper discusses a procedure for fast and simple surrogate-based yield optimization of high-frequency structures. The main concept of the approach is a tailored definition of the surrogate domain, which is based on a couple of pre-optimized designs that reflect the directions featuring maximum variability of the circuit responses with respect to its dimensions. A compact size of such a domain allows for the construction of an accurate metamodel therein using moderate numbers of training samples, and subsequently, it is employed to enhance the yield. The implementation details are dedicated to a particular type of device. Results obtained for a ring-slot antenna and a miniaturized rat-race coupler imply that the cost of yield optimization process can be reduced to few dozens of EM analyses.

Keywords: statistical analysis; yield optimization; metamodeling; performance-driven modeling; domain confinement



Citation: Koziel, S.; Pietrenko-Dabrowska, A. Performance-Driven Yield Optimization of High-Frequency Structures by Kriging Surrogates. *Appl. Sci.* **2022**, *12*, 3697. <https://doi.org/10.3390/app12073697>

Academic Editors: Jérôme Morio and Amalia Miliou

Received: 8 February 2022

Accepted: 29 March 2022

Published: 6 April 2022

Publisher's Note: MDPI stays neutral with regard to jurisdictional claims in published maps and institutional affiliations.



Copyright: © 2022 by the authors. Licensee MDPI, Basel, Switzerland. This article is an open access article distributed under the terms and conditions of the Creative Commons Attribution (CC BY) license (<https://creativecommons.org/licenses/by/4.0/>).

1. Introduction

High-frequency systems are normally designed in the nominal sense, with possible deviations of geometry and material parameters (e.g., due to fabrication inaccuracies) being generally neglected. Yet, uncertainties may have detrimental effects on the performance. As a consequence, it is important to develop procedures for their evaluation. Among possible types of uncertainties, those pertinent to imperfect manufacturing [1,2] play the most important role in practice. They are stochastic, which makes statistical analysis imperative for their evaluation [3–5]. Diminishing the impact of parameter deviations requires a maximization of appropriately defined figures of merit such as response variance or the yield [6–8]. In the case of high-frequency systems, yield seems to be more suitable because performance specifications are often expressed in a minimax form, particularly for lower/upper acceptance thresholds for *S*-parameters, etc. [9–12].

As mentioned earlier, the evaluation of the effects of parameter tolerances involves statistical analysis [13,14]. For reliability, it is normally carried out using full-wave electromagnetic (EM) analysis, which is associated with significant computational costs. Nevertheless, it is mandatory whenever simpler models (e.g., equivalent circuits) fail insufficiently to account for cross-coupling and similar effects [15–18]. Improving the computational efficiency of statistical analysis can be achieved using simplistic yet inaccurate methods

(e.g., worst-case analysis [19–21]) or surrogate-assisted techniques [22,23], where repetitive EM simulations are replaced by an evaluation of a fast replacement model, usually prepared beforehand. Popular modeling methods include polynomial approximation [24], neural networks (NNs) [25,26], or polynomial chaos expansion (PCE) [27–33]. Despite their advantages, surrogate-based methods are affected by the curse of dimensionality, resulting in excessive costs of model rendition for more complex systems. The alleviation of these difficulties is partially possible by the employment of hybrid techniques (e.g., PC kriging [6,34,35]), dimensionality reduction [36], multi-resolution methods (space mapping [37–40] and co-kriging [41,42]), or model order reduction [43].

Reducing the effects of manufacturing tolerances is even more essential than their evaluation. The relevant procedures are often referred to as robust design (also yield-driven design, tolerance-aware optimization, etc.) [1,44–47]. In practical terms, this can be accomplished by improving the statistical merit functions of choice, such as the yield. Unfortunately, yield maximization is a CPU-heavy task to the extent of being prohibitive when directly executed at the level of EM simulation models. Surrogate-assisted procedures offer viable workarounds [6,24–28]. Some of the most popular modeling methods utilized in this context are polynomial approximations [24], space mapping [48], NNs [49], and PCE [50]. As for statistical analysis, the bottleneck is a potentially high cost of the surrogate model setup, related to the dimensionality of the parameter space and parameter ranges. A partial mitigation has been offered by sequential approximation optimization (SAO) [51], where the metamodel is rendered along the optimization path, within the limited-volume domains centered at the current design produced by the robust design procedure. Another option is to employ response-feature technology [52]. This method capitalizes on the reduced nonlinearity of the relationship between the appropriately selected characteristic points of the system's responses and geometry parameters of the structure under design. The latter enables the construction of accurate metamodels using small training datasets [53].

In this work, we discuss a method for reduced-expense yield maximization of antenna and microwave components. Our approach involves the recently introduced performance-driven (or constrained) modeling [54–56], which addresses the surrogate construction task from the perspective of the model domain. More specifically, the model is only rendered in the vicinity of the region containing high-quality designs, which prevents wasting computational resources in parameter space regions containing uninteresting designs. This approach enables the construction of reliable metamodels over broad ranges of parameters and operating conditions using limited numbers of training data points [57–59]. Here, this paradigm is employed to construct surrogate models for robust design purposes. In particular, the domain of such a surrogate is extended along the directions possessing a major impact on the system's yield (the directions are found using a separate optimization sub-problems) and restricted along the remaining directions. Low domain volumes allow us to construct reliable surrogates, which are sufficient for conducting the yield maximization process without the necessity to rebuild the model. Our methodology is demonstrated using a ring-slot antenna and a microstrip coupler. In both cases, the robust design process is accomplished at a cost corresponding to less than a hundred of EM simulations. Reliability is corroborated by using EM-driven Monte Carlo analysis.

2. Yield Optimization Problem and Benchmark Algorithms

This section recalls the yield optimization problem statement, illustrated using two specific cases, multi-band antennas, and equal power split coupler. Subsequently, two basic state-of-the-art surrogate-assisted yield optimization algorithms are described. These will be used as benchmark methods in Section 4.

2.1. Yield Optimization Problem

In antenna and microwave designs, performance requirements are frequently formulated in a minimax form, i.e., by setting upper/lower acceptance levels on the electrical characteristics of the device at hand. These may include maximum in-band reflection

(antennas) or maximum power split error within the operating band (couplers) [9]. As a consequence, a commonly utilized figure of merit is the yield [4], i.e., the percentage of designs for which the target specifications are met given the assumed deviations of the parameters. Figures 1 and 2 show two examples of the design optimization tasks of high-frequency devices: a multi-band antenna and a microwave coupler. The figures provide the design specifications, as well as the formulations of the respective objective functions. For the antenna, the nominal design has to ensure the best possible matching within the operating bands of interest, whereas in the case of the coupler, the aim is to ensure equal power split and to improve the bandwidth. Typically, the nominal designs serve as a starting point for yield optimization.

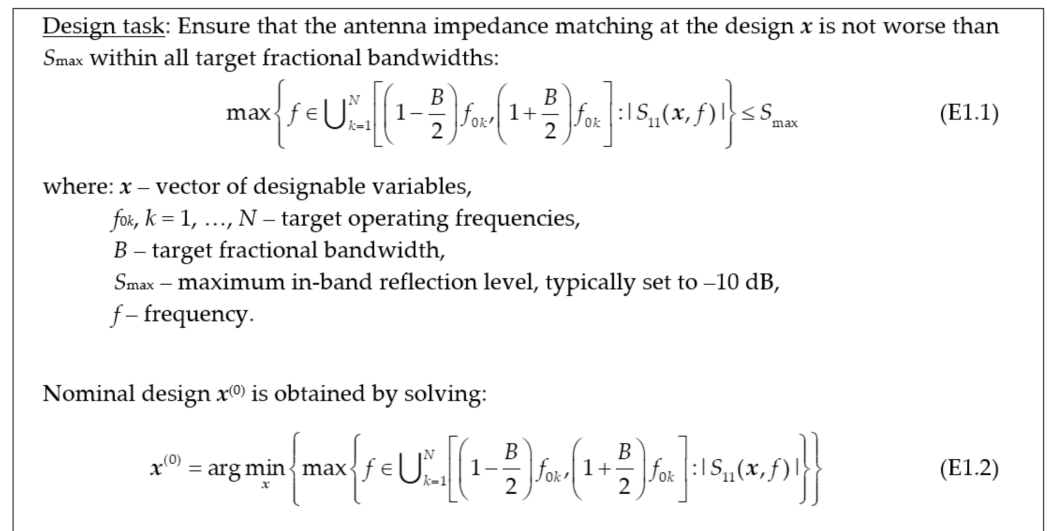


Figure 1. Example I: Multiple-band antenna optimized for best in-band matching.

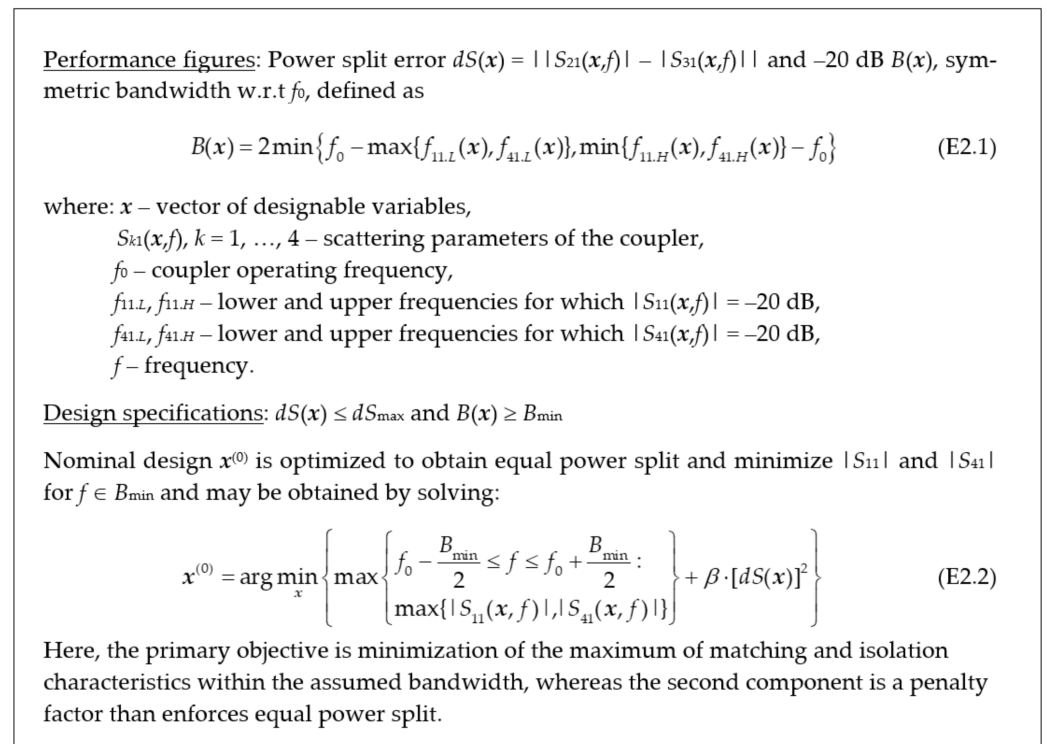


Figure 2. Example II: Microwave coupler optimized to ensure the target power split and bandwidth enhancement.

The deviations dx (e.g., manufacturing tolerances) are characterized by the specified probability distributions (e.g., uniform of maximum deviation δ_{\max} or joint Gaussian $N(0,\sigma)$). The deviations may be correlated [60], yet we assume here that they are statistically independent. Yield $Y(x)$ at a certain the design x may be assessed by using Monte Carlo analysis.

$$Y(x) = \frac{1}{p} \sum_{k=1}^p H(x^{(k)}) \tag{1}$$

In (1), $x^{(k)} = x + dx^{(k)}$, $k = 1, \dots, p$, denote the observables, $dx^{(k)}$ are the random deviations, and $H(x)$ is given by the following.

$$H(x) = \begin{cases} 1 & \text{if design specifications are satisfied} \\ 0 & \text{otherwise} \end{cases} \tag{2}$$

We employ the following formulation of the yield optimization task.

$$x^* = \underset{x}{\operatorname{argmin}} \{-Y(x)\} \tag{3}$$

Commonly, nominal design $x^{(0)}$ is used as a starting point for solving (3), which, in turn, is rendered by solving, e.g., problem (E1.2) (for the example of the multi-band antenna) or (E2.2) (for the example of the microwave coupler).

2.2. Yield Optimization. Benchmark Surrogate-Assisted Algorithms

This section delineates the benchmark surrogate-assisted techniques: one-shot approach (Algorithm 1) and sequential approximate optimization SAO (Algorithm 2), the main features of which are juxtaposed in Table 1. Algorithms 1 and 2 exploit kriging data-driven surrogates [61], yet the actual choice of metamodeling technique is of secondary importance (other possibilities are, e.g., RBF [62] or PCE [29]).

Table 1. Surrogate-assisted yield optimization: one-shot approach and sequential approximate optimization.

Algorithm	Algorithm 1	Algorithm 2
Method	One-shot approach	Sequential approximate optimization
Solving optimization task	Solve a single task $x^* = \operatorname{argmin}\{x \in X_S: -Y(x)\}$ within the surrogate domain X_S	Render series $x^{(i)}$, $i = 0, 1, \dots$, of approximations to x^* by solving $x^{(i+1)} = \operatorname{argmin}\{x \in X_{S,i}: -Y_s^{(i)}(x)\}$
Yield estimation	$Y(x)$ evaluated once using single surrogate	In each iteration, $Y_s^{(i)}$ is evaluated using the i th surrogate
Surrogate domain	$X_S = [x^{(0)} - \delta, x^{(0)} + \delta]$, $\delta = [\delta_1 \dots \delta_n]^T$, $\delta_k = 10\delta_{\max}^\#, k = 1, \dots, n$	$X_{S,i} = [x^{(i)} - \delta, x^{(i)} + \delta]$, $\delta = [\delta_1 \dots \delta_n]^T$, $\delta_k = 3\delta_{\max}^\#, k = 1, \dots, n$
Pros	Simple to apply	Reduced cost of setting up the surrogate (smaller domain)
Cons	Expected high cost of surrogate construction in a larger domain	Iterative process involving domain relocation and constructing several surrogates

[#] δ_{\max} —maximum deviation for uniform distribution (or 3σ for Gaussian distribution of variance σ).

The overall idea of Algorithm 1 is to build a single surrogate for which its domain is spread over an ample neighborhood of the nominal design solution, within which the yield may be estimated in a reliable manner. This method is unsophisticated; however, the training data acquisition cost may be sizeable (proportional to the domain size). On the other hand, in Algorithm 2, yield estimation is replaced by an iterative process. Here, the aim is to set up the metamodel over a domain of a lower size, and then reposition it from iteration to iteration. Consequently, the CPU cost of the surrogate setup is reduced

(as compared to Algorithm 1); however, the optimization process typically takes several iterations to converge.

3. Surrogate-Based Yield Optimization with Domain Confinement

This section discusses the main components of the considered optimization framework that preserves the simplicity of the one-shot approach (Algorithm 1), while keeping the surrogate setup cost at a reasonable level. This is achieved by exploiting the performance-driven modeling paradigm [54,55]. The employed procedure for locating the directions that span the metamodel domain is introduced in the context of multi-band antenna designs (Section 3.1) and microwave coupler designs (Section 3.2), along with the respective domain definitions. These two methods share the same underlying idea, yet they are tailored to the particular sets of performance specifications, as delineated in Section 2.1.

3.1. Yield Optimization of Multi-Band Antennas

The directions that affect the antenna characteristics to the highest degree are selected by pre-optimizing two supplementary designs: (i) the design that maximizes the antenna symmetrical fractional bandwidths, and (ii) the design that minimizes the antenna reflection at $f_{0,k}, k = 1, \dots, N$, (i.e., the resonant frequencies). These designs are rendered by solving the following [63].

$$\mathbf{x}^{(1)} = \operatorname{argmin}_x \{-\min\{B_1(\mathbf{x}), \dots, B_N(\mathbf{x})\}\} \tag{4}$$

$$\mathbf{x}^{(2)} = \operatorname{argmin}_x \{\max\{|S_{11}(\mathbf{x}, f_{01})|, \dots, |S_{11}(\mathbf{x}, f_{0N})|\}\} \tag{5}$$

In (4), $B_k(\mathbf{x}) = 2\min\{f_{0k} - f_{1k}(\mathbf{x}), f_{2k}(\mathbf{x}) - f_{0k}\}, k = 1, \dots, N$, (symmetric portion of the bandwidth), whereas f_{1k} and f_{2k} denote the frequencies for which $|S_{11}|$ assumes -10 dB level (the lower and higher frequencies around the k th resonance). The trust-region gradient algorithm [64] is employed to solve problems (4) and (5), and the antenna response sensitivities are updated by applying the Broyden formula [65]. Consequently, the optimization cost equals approximately $1.5n$ EM analyses (n being the number of designable parameters).

Figure 3 describes surrogate domain X_S and its establishment with the use of the reference designs, whereas Figure 4 illustrates this process graphically. The surrogate domain X_S is small; still, it encompasses the most consequential directions of antenna response variations that directly affect the yield, thereby allowing for significant cost reductions. The yield is optimized directly by solving (3) (i.e., the surrogate is used instead of EM simulations), similarly as in Algorithm 1.

Let $\mathbf{s}(t) = [s_1(t) \dots s_n(t)]^T$ be a t -parameterized curve such that the following is the case:

$$s_j(t) = a_{j0} + a_{j1}t + a_{j2}t^2$$

for $0 \leq t \leq 1$, so that $\mathbf{s}(0) = \mathbf{x}^{(1)}, \mathbf{s}(0.5) = \mathbf{x}^{(0)}$, and $\mathbf{s}(1) = \mathbf{x}^{(2)}$.

The model coefficients can be found as follows.

$$\begin{bmatrix} a_{10} & L & a_{n0} \\ a_{11} & L & a_{n1} \\ a_{12} & L & a_{n2} \end{bmatrix} = \begin{bmatrix} 1 & 0 & 0 \\ 1 & 0.5 & 0.25 \\ 1 & 1 & 1 \end{bmatrix}^{-1} \begin{bmatrix} (\mathbf{x}^{(1)})^T \\ (\mathbf{x}^{(0)})^T \\ (\mathbf{x}^{(2)})^T \end{bmatrix}$$

Let $S(t)$ be the interval with the center at $\mathbf{s}(t)$ and the size $\delta_c = [\delta_{c1} \dots \delta_{cn}]^T$, where δ_{cj} is a small multiplicity of the maximum design deviation δ_{\max} , e.g., $2\delta_{\max}$.

Surrogate model domain X_S is defined as the set-theory union of the intervals $S(t)$ for $0 \leq t \leq 1$.

$$X_S = \bigcup_{0 \leq t \leq 1} S(t)$$

X_S contains the reference designs $\mathbf{x}^{(0)}, \mathbf{x}^{(1)}$, and $\mathbf{x}^{(2)}$ and a vicinity of the entire curve $\mathbf{s}(t)$ of size δ .

Figure 3. Surrogate domain definition using the reference designs. Multi-band antennas case.

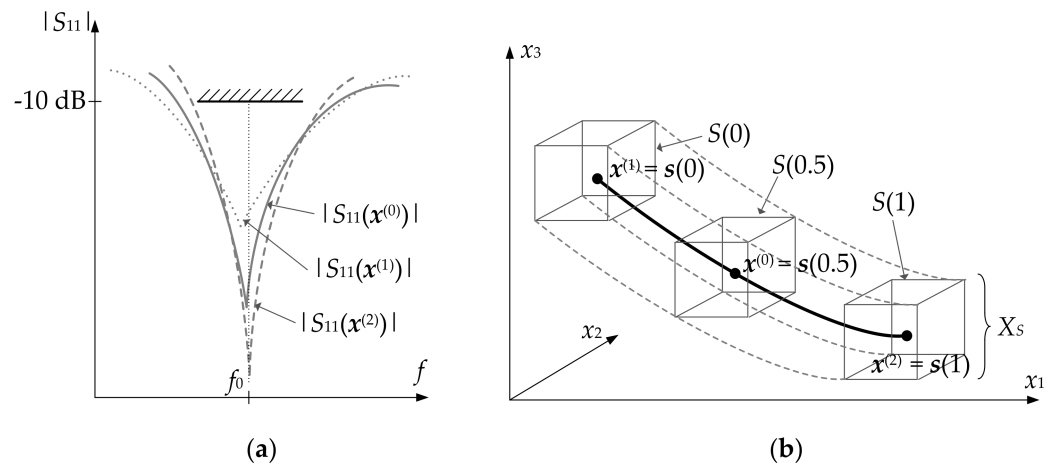


Figure 4. Yield optimization of multi-band antennas using performance-driven surrogates: (a) reflection responses of an exemplary narrow-band antenna at the nominal design $\mathbf{x}^{(0)}$, maximum bandwidth design $\mathbf{x}^{(1)}$, and best matching (at f_0) design $\mathbf{x}^{(2)}$. These designs determine the directions of the most significant response changes (from the point of view of the target operating bandwidth); (b) The reference designs $\mathbf{x}^{(0)}$ through $\mathbf{x}^{(2)}$ form a path (a parameterized curve $s(t)$). The union of intervals $S(t)$ (cf. (15)) form the surrogate model domain X_S .

3.2. Yield Optimization of Microwave Couplers

In this case, the design requirements include the power split error and the bandwidth. We define $f_{11.L}(\mathbf{x}), f_{11.H}(\mathbf{x}), f_{41.L}(\mathbf{x})$, and $f_{41.H}(\mathbf{x})$ (the frequencies that are bandwidth boundaries) and also $l_1(\mathbf{x}) = |S_{21}(\mathbf{x}, f_0)|$ and $l_2(\mathbf{x}) = |S_{31}(\mathbf{x}, f_0)|$ (the levels of the respective coupler responses at its operating frequency). These, in turn, are gathered in the vector $F(\mathbf{x}) = [f_{11.L}(\mathbf{x}), f_{11.H}(\mathbf{x}), f_{41.L}(\mathbf{x}), f_{41.H}(\mathbf{x}), l_1(\mathbf{x}), l_2(\mathbf{x})]^T$, for which Jacobian J_F can be derived from the Jacobian J_S of the circuit response (evaluated through finite differentiation). The linear expansion model of F at the nominal design $\mathbf{x}^{(0)}$ is as follows [66].

$$L_F(\mathbf{x}) = [L_1(\mathbf{x})L_2(\mathbf{x}) \dots L_6(\mathbf{x})]^T = F(\mathbf{x}^{(0)}) + J_F(\mathbf{x}^{(0)}) \cdot (\mathbf{x} - \mathbf{x}^{(0)}) \tag{6}$$

As before, we also have two supplementary designs $\mathbf{x}^{(1)}$ and $\mathbf{x}^{(2)}$ yielded by solving the following.

$$\mathbf{x}^{(1)} = \operatorname{argmin}_{\mathbf{x}} \left\{ L_5(\mathbf{x}) - L_6(\mathbf{x}) + \beta_2 \left\| \begin{bmatrix} L_1(\mathbf{x}) \\ \vdots \\ L_4(\mathbf{x}) \end{bmatrix} - \begin{bmatrix} L_1(\mathbf{x}^{(0)}) \\ \vdots \\ L_4(\mathbf{x}^{(0)}) \end{bmatrix} \right\|^2 \right\} \tag{7}$$

$$\mathbf{x}^{(2)} = \operatorname{argmin}_{\mathbf{x}} \left\{ -2\min\{f_0 - \max\{L_1(\mathbf{x}), L_3(\mathbf{x})\}, \min\{L_2(\mathbf{x}), L_4(\mathbf{x})\} - f_0\} + \beta_1 \cdot [L_5(\mathbf{x}) - L_6(\mathbf{x})]^2 \right\} \tag{8}$$

Both (7) and (8) are subject to $\|\mathbf{x} - \mathbf{x}^{(0)}\| \leq D$ (D being selected by the user; here, we set $D = 0.5$ mm). Solving (7) and (8) requires merely n EM analyses of the coupler (it is the cost of estimating J_F in (6)). These designs serve to find the directions corresponding to the maximal variations of the coupler power split and bandwidth, respectively. Figure 5 provides a brief description of the surrogate domain definition using these reference designs, whereas a graphical illustration of these procedure is provided in Figure 6.

Let $S(\mathbf{t}) = [S_1(\mathbf{t}) \dots S_n(\mathbf{t})]^T$ be a \mathbf{t} -parameterized surface such that

$$S(\mathbf{t}) = S([t_1 \ t_2]^T) = \mathbf{x}^{(0)} + t_1 \mathbf{v}_1 + t_2 \mathbf{v}_2$$

for $-1 \leq t_1, t_2 \leq 1$. We have $S([0 \ 0]^T) = \mathbf{x}^{(0)}$, $S([1 \ 0]^T) = \mathbf{x}^{(1)}$, and $S([0 \ 1]^T) = \mathbf{x}^{(2)}$.

Let $S_i(\mathbf{t})$ be the interval with the centre at $S(\mathbf{t})$ and the size $\delta = [\delta_1 \dots \delta_n]^T$, where δ_j is a multiplicity of the maximum design deviation δ_{\max} , e.g., $2\delta_{\max}$.

The surrogate model domain X_S is then defined as the union of all intervals $S_i(\mathbf{t})$ for $-1 \leq t_1, t_2 \leq 1$, i.e.,

$$X_S = \bigcup_{-1 \leq t_1, t_2 \leq 1} S_i([t_1 \ t_2]^T)$$

Figure 5. Surrogate domain definition using the reference designs. Microwave couplers case.

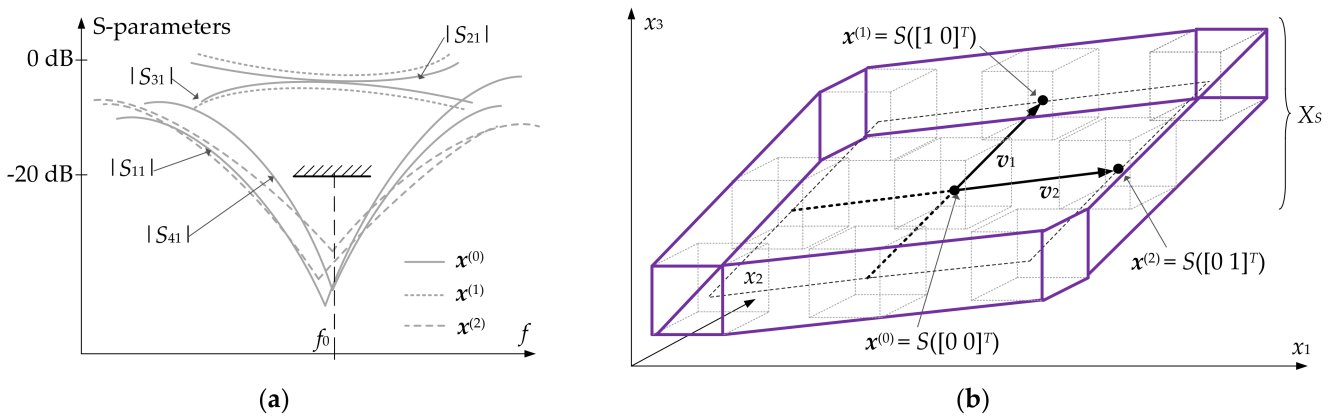


Figure 6. Yield optimization of microwave couplers by means of performance-driven surrogates: (a) scattering parameters of an exemplary coupler at the nominal design $\mathbf{x}^{(0)}$, design $\mathbf{x}^{(1)}$ (spoiled power split), and design $\mathbf{x}^{(2)}$ (improved -20 dB bandwidth); for clarity, only the selected S-parameters are shown for $\mathbf{x}^{(1)}$ ($|S_{21}|$, $|S_{31}|$) and $\mathbf{x}^{(2)}$ ($|S_{11}|$, $|S_{41}|$). These designs determine the directions of the most significant response changes (from the point of view of yield manipulation). (b) The designs $\mathbf{x}^{(0)}$ to $\mathbf{x}^{(2)}$ form a parameterized surface $S(\mathbf{t})$. The union of intervals $S_i(\mathbf{t})$ (cf. (21)) forms surrogate model domain X_S .

Surrogate domain X_S is small volume-wise, yet it is ample enough to encompass the directions of essential changes of the coupler responses affecting its yield. As in the previous case (Section 3.1), a small volume of the domain allows a significant reduction in the cost of setting up the surrogate, and also—due to the mentioned coverage of important directions—there is no need to iterate the entire process (as in Algorithm 2). The yield optimization process is conducted by solving (3), i.e., similarly as in the algorithm of Section 3.1.

4. Demonstration Case Studies

This section provides the results obtained using the algorithms of Sections 3.1 and 3.2 using a ring-slot antenna, and a miniaturized rat-race coupler as verification structures. The procedure is benchmarked against the surrogate-assisted approaches of Section 2. In order to verify the reliability of the considered methodology, a Monte Carlo analysis has been executed at the nominal design and the yield maximizing design.

4.1. Case I: Ring-Slot Antenna

Figure 7 shows our first verification structure: a ring slot antenna, for which its circular ground plane featuring a slot with defected ground structure is excited through a microstrip line [67], whereas all the pertinent details are provided in Figure 8. We assumed independent uniformly distributed parameter deviations with maximum deviation $\delta_{\max} = 0.05$ mm. The yield optimization results are provided in Table 2 for the algorithm of Section 3.1 and the benchmark surrogate-assisted procedures of Table 1. For the discussed approach, the size of the metamodel domain was set to $\delta_{c,k} = 2\delta_{\max}$ (see Figure 3); the training data set for constructing the surrogate contained 35 samples; and its relative RMS error equals 0.5%.

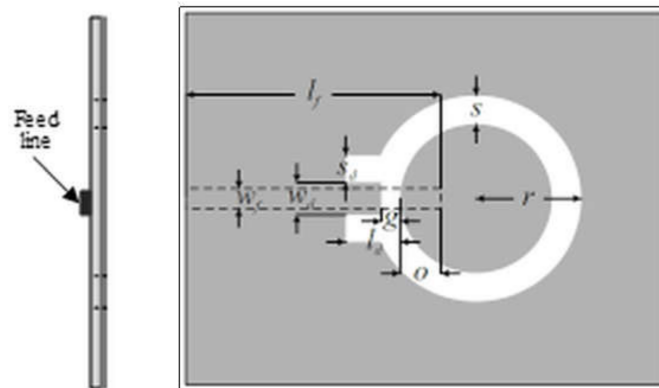


Figure 7. Geometry of the ring slot antenna with a microstrip feed (dashed line) [67].

Ring slot antenna:

Substrate: $h = 0.76$ mm, relative permittivity $\epsilon = 2.0$

Geometry parameters: $\mathbf{x} = [l_f \ l_s \ w \ r \ s \ a \ o \ g]^T$

Design objective: minimization of the in-band reflection for the frequency range 4.15 GHz to 4.85 GHz (center frequency $f_0 = 4.5$ GHz)

The nominal design: $\mathbf{x}^{(0)} = [20.28 \ 6.54 \ 0.24 \ 11.83 \ 2.95 \ 6.77 \ 7.85 \ 2.23]^T$

Reference designs (yielded at the cost of only 13 and 14 EM simulations, respectively):

$\mathbf{x}^{(1)} = [20.03 \ 6.30 \ 0.20 \ 11.84 \ 2.94 \ 6.74 \ 7.89 \ 2.43]^T$ (maximum bandwidth (4))

$\mathbf{x}^{(2)} = [20.26 \ 6.51 \ 0.20 \ 11.68 \ 2.92 \ 6.47 \ 7.49 \ 2.24]^T$ (best reflection at $f_0 = 4.5$ GHz (5))

Figure 8. Description of the ring slot antenna of Figure 7 [67].

Table 2. Yield optimization of the ring-slot antenna of Figure 7.

Optimization Algorithm	Initial Yield		Optimized Yield		CPU Cost [§]
	Estimated by Metamodel	EM-Based	Estimated by Metamodel	EM-Based	
Algorithm 1	81%	81%	92%	93%	400
Algorithm 2	81%	81%	91%	91%	150 [#]
Algorithm of Section 3.1	81%	81%	91%	91%	62 ^{&}

[§] Optimization cost in number of EM analyses of the antenna structure. [#] The algorithm convergence after four iterations (surrogate setup cost 100 training samples per iteration). [&] The cost includes training data acquisition (35 EM analyzes) and the generation of reference designs $\mathbf{x}^{(1)}$ and $\mathbf{x}^{(2)}$ (27 EM simulations in total).

The details pertaining to the benchmark procedures are as follows. For Algorithm 1, the metamodel of relative RMS error 0.7% was constructed using 400 samples within the domain of size $10\delta_{\max}$. For Algorithm 2, the surrogate models were built using 50 training data samples over the domain of size $3\delta_{\max}$. Here, the first metamodel (of the domain focused around $\mathbf{x}^{(0)}$) featured a relative RMS error of 0.4%. In both cases, the aim was to

render the metamodels of similar accuracy to less than one percent to ensure the reliability of the yield estimation. The following yield maximizing design was rendered $x^* = [20.18 \ 6.43 \ 0.21 \ 11.85 \ 2.95 \ 6.78 \ 7.90 \ 2.31]^T$. Figure 9 visualizes the results of Monte Carlo analysis at $x^{(0)}$ and at x^* (carried out with the use of 500 samples).

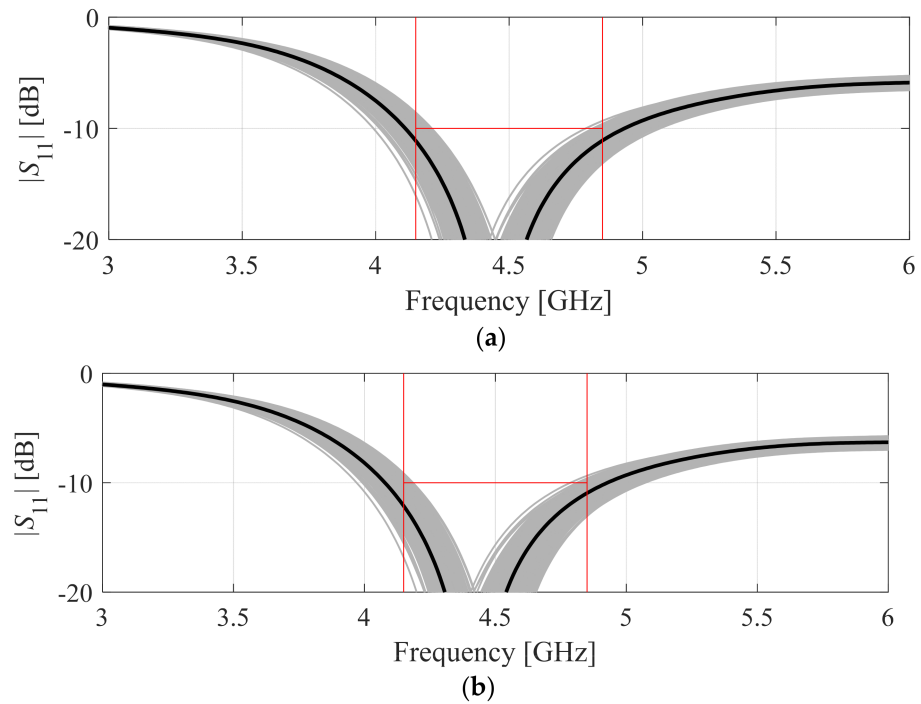


Figure 9. Monte Carlo analysis of antenna of Figure 7 using EM simulations (gray plots): (a) nominal design; (b) yield-optimized design obtained using the algorithm of Section 3.1. Black plots show the antenna response at the nominal and optimized designs, respectively.

The results of Table 2 may be summarized as follows. The metamodel domain confinement according to the methodology described in Section 3.1. results in dramatic cost savings, which is mainly due to the decreased volume size. Still, as the domain is spanned over the significant directions of the design space (those representing the maximum variations of the antenna response), the yield optimization process may successfully be concluded in one stage.

4.2. Case IV: Compact Microstrip Rat-Race Coupler

The second verification structure is a miniaturized microstrip rat-race coupler (RRC) presented in Figure 10 and described in Figure 11 [68]. The compact size of the circuit is a result of folding of the transmission lines that constitute its interior.

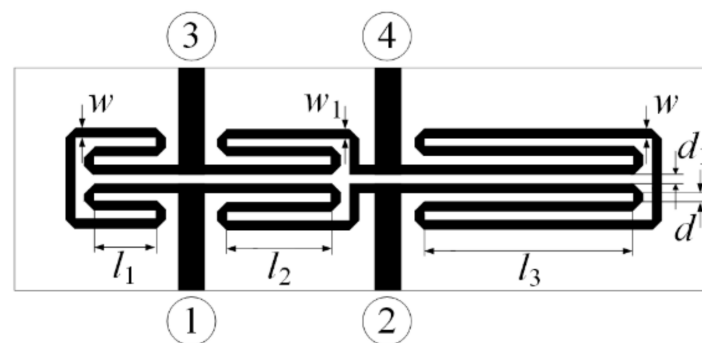


Figure 10. Layout of the miniaturized folded rat-race coupler [68]; the numbered circles (1 through 4) mark the structure ports.

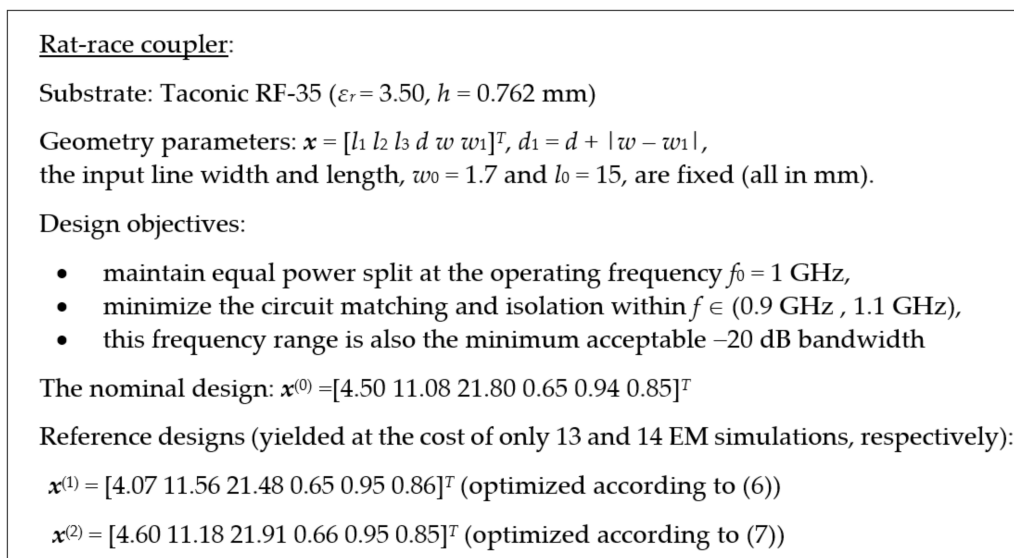


Figure 11. Description of the rat-race coupler of Figure 10 [68].

Parameter deviations are assumed to be independently and uniformly distributed with the maximum deviation of $\delta_{\max} = 0.05$ mm. For the discussed algorithm, the metamodel of the relative RMS error of 2.3% was set up within a domain of size $\delta_{c,k} = 2\delta_{\max}$, and the training data set comprised 72 training samples. In the case of Algorithm 1, the surrogate was constructed with 400 samples allocated over the domain of size $10\delta_{\max}$, and the relative RMS error was equal to 3.4%. For Algorithm 2, the first metamodel set up with 50 samples within the domain encompassing $\mathbf{x}^{(0)}$ featured a relative RMS error of 2.2% (the size-defining parameter has been set to $3\delta_{\max}$). Table 3 provides the relevant results for the discussed and benchmark algorithms. The following optimal design was yielded: $\mathbf{x}^* = [4.65 \ 11.10 \ 21.87 \ 0.71 \ 0.95 \ 0.81]^T$.

Table 3. Yield optimization of the compact coupler of Figure 10.

Optimization Algorithm	Initial Yield		Optimized Yield		CPU Cost [§]
	Estimated by Metamodel	EM-Based	Estimated by Metamodel	EM-Based	
Algorithm 1	67%	62%	90%	83%	400
Algorithm 2	66%	62%	86%	83%	200 [#]
Algorithm of Section 3.1	63%	62%	84%	82%	72

[§] Optimization cost in number of EM analyses of the antenna structure. [#] Algorithm convergence after four iterations (surrogate setup cost 100 training samples per iteration).

The results of Monte Carlo analysis at the initial and optimal designs are shown in Figure 12 (500 uniformly distributed samples were used with $\delta_{\max} = 0.05$ mm). In this case, the discussed approach and Algorithm 2 were able to estimate the yield in a reliable manner. As for Algorithm 1, the values of the yield predicted using the surrogate and EM simulations differed considerably. This is because the surrogate rendered across a domain of a larger size featured worse predictive power.

As in the previous case, it has been verified that the yield optimization within a confined domain enables the obtainment of the benefits of both benchmark procedures. Thus, the entire process may be concluded in one stage due to spanning the domain along the most consequential directions (as opposed to the iterative Algorithm 2). Moreover, as the domain is of reduced size, it was possible to construct the surrogate at a remarkably low cost. The computational savings reached up to 82 and 64 percent (the discussed procedure versus Algorithms 1 and 2, respectively). At the same time, high design quality was maintained in all cases, and the value of the optimized yield is similar for all compared algorithms. Furthermore, the obtained results agree with those of EM-based Monte Carlo analysis.

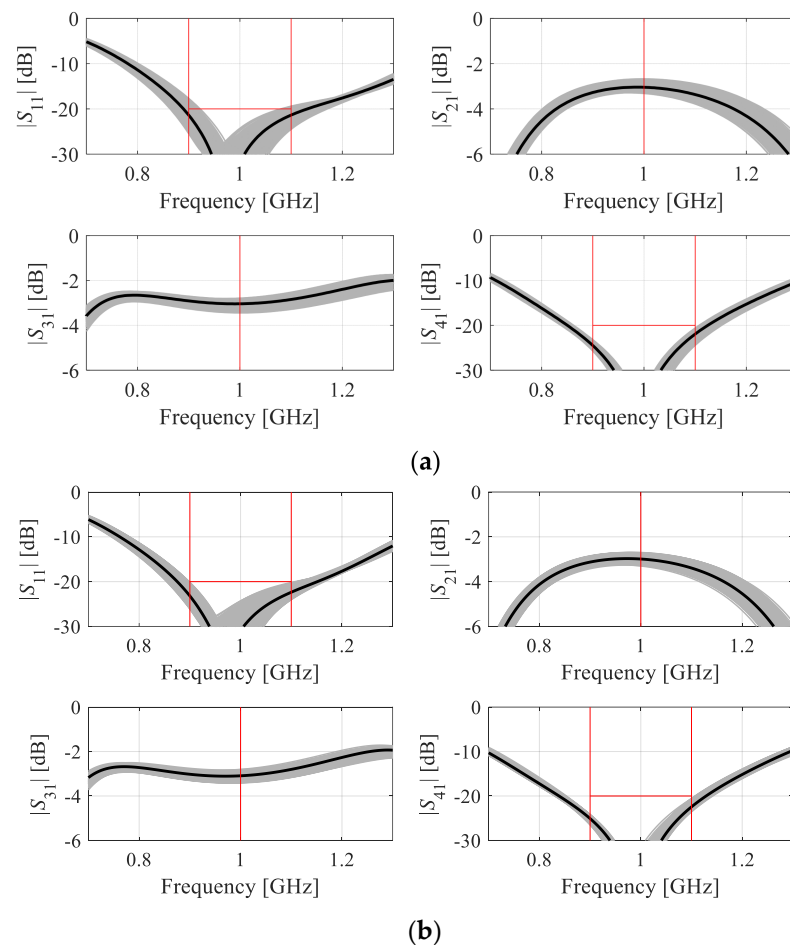


Figure 12. Monte Carlo analysis of the coupler of Figure 10 using EM simulations (gray plots): (a) nominal design; (b) yield-optimized design obtained using the algorithm of Section 3.2. Black plots show the antenna response at the nominal and the optimized designs, respectively.

5. Conclusions

This work discussed the recent techniques for surrogate-based yield maximization of high-frequency components. The main ingredients of the optimization framework are domain-confined metamodels constructed by keeping in mind the parameter-space directions that are the most influential in terms of affecting the system's performance. By maintaining the low overall volume of the domain, it is possible to construct reliable surrogates using a limited number of training data samples, and it is possible to carry out the yield optimization process without the need to rebuild the model. As demonstrated using two microstrip structures (an antenna and a rat-race coupler), the robust design process can be accomplished at remarkably low costs of a few dozens of EM simulations. Thorough benchmarking indicates significant savings, with >80 percent over reference surrogate-based approach and >60 percent over the SAO algorithm. At the same time, reliability has been corroborated using EM-driven Monte Carlo simulations. The optimization techniques considered in the paper offer improved computational efficiency over the state-of-the-art methods without compromising reliability. They are applicable to a variety of antenna and microwave components, and they may be viewed as potential replacements of conventional (also surrogate-assisted) procedures, especially for more complex, e.g., higher-dimensional design scenarios. Since in the considered approach, the surrogate domain is spanned by the directions that influence yield values in the most significant manner, the generalization of the technique would require properly defining these directions so that they reflect the respective design requirements.

In general, the two specific approaches for constructing the domain of the surrogate model (extension along the one-dimensional curve for the antenna example, and along two vectors corresponding to the maximum changes of the considered performance figures for the coupler example) could be applied to either of the case studies. However, maintaining the domain extension's dimensionality as equal to the number of considered performance figures is recommended, which is to provide sufficient room for yield improvement within the domain.

Author Contributions: Conceptualization, A.P.-D. and S.K.; methodology, A.P.-D. and S.K.; software, A.P.-D.; validation, A.P.-D. and S.K.; formal analysis, A.P.-D. and S.K.; investigation, A.P.-D.; resources, S.K.; data curation, A.P.-D.; writing—original draft preparation, A.P.-D. and S.K.; writing—review and editing, A.P.-D. and S.K.; visualization, A.P.-D.; supervision, S.K.; project administration, S.K.; funding acquisition, S.K. All authors have read and agreed to the published version of the manuscript.

Funding: This work was supported in part by the Icelandic Centre for Research (RANNIS), Grant 206606, and by National Science Centre of Poland, Grant 2018/31/B/ST7/02369.

Institutional Review Board Statement: Not applicable.

Informed Consent Statement: Not applicable.

Data Availability Statement: Not applicable.

Acknowledgments: The authors thank Dassault Systemes, France, for making CST Microwave Studio available.

Conflicts of Interest: The authors declare no conflict of interest. The funders had no role in the design of the study; in the collection, analyses, or interpretation of data; in the writing of the manuscript; or in the decision to publish the results.

References

1. Biernacki, R.; Chen, S.; Estep, G.; Rousset, J.; Sifri, J. Statistical analysis and yield optimization in practical RF and microwave systems. In Proceedings of the 2012 IEEE/MTT-S International Microwave Symposium Digest, Montreal, QC, Canada, 17–22 June 2012; pp. 1–3.
2. Liang, J.F.; Chang, H.C.; Zaki, K.A. Design and tolerance analysis of thick iris waveguide bandpass filters. *IEEE Trans. Magn.* **1993**, *29*, 1605–1609. [[CrossRef](#)]
3. Hassan, A.S.O.; Abdel-Malek, H.L.; Mohamed, A.S.A.; Abuelfadl, T.M.; Elqenawy, A.E. Statistical design centering of RF cavity linear accelerator via non-derivative trust region optimization. In Proceedings of the 2015 IEEE MTT-S International Conference on Numerical Electromagnetic and Multiphysics Modeling and Optimization (NEMO), Ottawa, ON, Canada, 11–14 August 2015; pp. 1–3.
4. Koziel, S.; Bandler, J.; Mohamed, A.; Madsen, K. Enhanced surrogate models for statistical design exploiting space mapping technology. In Proceedings of the IEEE MTT-S International Microwave Symposium Digest, Long Beach, CA, USA, 17 June 2015; pp. 1–4.
5. Syrytsin, I.; Zhang, S.; Pedersen, G.F.; Zhao, K.; Bolin, T.; Ying, Z. Statistical investigation of the user effects on mobile terminal antennas for 5G applications. *IEEE Trans. Ant. Prop.* **2017**, *65*, 6596–6605. [[CrossRef](#)]
6. Leifsson, L.; Du, X.; Koziel, S. Efficient yield estimation of multi-band patch antennas by polynomial chaos-based kriging. *Int. J. Numer. Modeling.* **2020**, *66*, e2722.
7. Prasad, A.K.; Ahadi, M.; Roy, S. Multidimensional uncertainty quantification of microwave/RF networks using linear regression and optimal design of experiments. *IEEE Trans. Microw. Theory Tech.* **2016**, *64*, 2433–2446. [[CrossRef](#)]
8. Kim, D.W.; Choi, N.S.; Lee, C.U.; Kim, D.H. Assessment of statistical moments of a performance function for robust design of electromagnetic devices. *IEEE Trans. Magn.* **2015**, *51*, 7205104. [[CrossRef](#)]
9. Budimir, D.; Goussetis, G. Design of asymmetrical RF and microwave bandpass filters by computer optimization. *IEEE Trans. Microw. Theory Tech.* **2003**, *51*, 1174–1178. [[CrossRef](#)]
10. Koziel, S.; Pietrenko-Dabrowska, A. Global EM-driven optimization of multi-band antennas using knowledge-based inverse response-feature surrogates. *Knowl.-Based Syst.* **2021**, *227*, 107189. [[CrossRef](#)]
11. Koziel, S.; Pietrenko-Dabrowska, A. Tolerance-aware multi-objective optimization of antennas by means of feature-based regression surrogates. *IEEE Trans. Ant. Prop.* **2022**. [[CrossRef](#)]
12. Pietrenko-Dabrowska, A.; Koziel, S. Design centering of compact microwave components using response features and trust regions. *Energies* **2021**, *14*, 8550. [[CrossRef](#)]
13. Vidal, B.; Corral, J.L.; Marti, J. Statistical analysis of WDM photonic microwave filters with random errors. *IEEE Trans. Microw. Theory Techn.* **2005**, *53*, 2600–2603. [[CrossRef](#)]

14. Li, X.; Zhou, J.; Duan, B.; Yang, Y.; Zhang, Y.; Fang, J. Performance of planar arrays for microwave power transmission with position errors. *IEEE Ant. Wirel. Prop. Lett.* **2015**, *14*, 1794–1797. [[CrossRef](#)]
15. Jin, H.; Zhou, Y.; Huang, Y.M.; Ding, S.; Wu, K. Miniaturized broadband coupler made of slow-wave half-mode substrate integrated waveguide. *IEEE Microw. Wirel. Comp. Lett.* **2017**, *27*, 132–134. [[CrossRef](#)]
16. Wu, H.W.; Chiu, C.T. Design of compact multi-layered quad-band bandpass filter. *IEEE Microw. Wirel. Comp. Lett.* **2016**, *26*, 879–881. [[CrossRef](#)]
17. Firmansyah, T.; Alaydrus, M.; Wahyu, Y.; Rahardjo, E.T.; Wibisono, G. A highly independent multiband bandpass filter using a multi-coupled line stub-SIR with folding structure. *IEEE Access* **2020**, *8*, 83009–83026. [[CrossRef](#)]
18. Chen, S.; Guo, M.; Xu, K.; Zhao, P.; Dong, L.; Wang, G. A frequency synthesizer based microwave permittivity sensor using CMRC structure. *IEEE Access* **2018**, *6*, 8556–8563. [[CrossRef](#)]
19. Sengupta, M.; Saxena, S.; Daldoss, L.; Kramer, G.; Minehane, S.; Cheng, J. Application-specific worst case corners using response surfaces and statistical models. *IEEE Trans. Comput.-Aided Design Integr. Circuits Syst.* **2005**, *24*, 1372–1380. [[CrossRef](#)]
20. Zhang, B.; Rahmat-Samii, Y. Robust optimization with worst case sensitivity analysis applied to array synthesis and antenna designs. *IEEE Trans. Ant. Prop.* **2018**, *66*, 160–171. [[CrossRef](#)]
21. Shen, H.; Xu, W.; Wang, J.; Zhao, C. A worst-case robust beamforming design for multi-antenna AF relaying. *IEEE Comm. Lett.* **2013**, *17*, 713–716. [[CrossRef](#)]
22. Ma, B.; Lei, G.; Liu, C.; Zhu, J.; Guo, Y. Robust tolerance design optimization of a PM claw pole motor with soft magnetic composite cores. *IEEE Trans. Magn.* **2018**, *54*, 8102404. [[CrossRef](#)]
23. Ren, Z.; He, S.; Zhang, D.; Zhang, Y.; Koh, C.S. A possibility-based robust optimal design algorithm in preliminary design state of electromagnetic devices. *IEEE Trans. Magn.* **2016**, *52*, 7001504. [[CrossRef](#)]
24. Matoglu, E.; Pham, N.; De Araujo, D.; Cases, M.; Swaminathan, M. Statistical signal integrity analysis and diagnosis methodology for high-speed systems. *IEEE Trans. Adv. Packag.* **2004**, *27*, 611–629. [[CrossRef](#)]
25. Zhang, L.; Zhang, Q.J.; Wood, J. Statistical neuro-space mapping technique for large-signal modeling of nonlinear devices. *IEEE Trans. Microw. Theory Tech.* **2008**, *56*, 2453–2467. [[CrossRef](#)]
26. Kim, D.; Kim, M.; Kim, W. Wafer edge yield prediction using a combined long short-term memory and feed-forward neural network model for semiconductor manufacturing. *IEEE Access* **2020**, *8*, 215125–215132. [[CrossRef](#)]
27. Du, J.; Roblin, C. Statistical modeling of disturbed antennas based on the polynomial chaos expansion. *IEEE Ant. Wirel. Prop. Lett.* **2017**, *16*, 1843–1847. [[CrossRef](#)]
28. Rossi, M.; Dierck, A.; Rogier, H.; Vande Ginste, D. A stochastic framework for the variability analysis of textile antennas. *IEEE Trans. Ant. Prop.* **2014**, *62*, 6510–6514. [[CrossRef](#)]
29. Petrocchi, A.; Kaintura, A.; Avolio, G.; Spina, D.; Dhaene, T.; Raffo, A.; Schreurs, D.M. Measurement uncertainty propagation in transistor model parameters via polynomial chaos expansion. *IEEE Microw. Wirel. Comp. Lett.* **2017**, *27*, 572–574. [[CrossRef](#)]
30. Zhang, Z.; Chen, H.; Yu, Y.; Jiang, F.; Cheng, Q.S. Yield-constrained optimization design using polynomial chaos for microwave filters. *IEEE Access* **2021**, *9*, 22408–22416. [[CrossRef](#)]
31. Klink, D.; Meyer, P.; Steyn, W. Efficient yield estimation of multiband patch antennas using NLPLS-based PCE. *IEEE Trans. Ant. Prop.* **2022**. [[CrossRef](#)]
32. Klink, D.; Meyer, P. A comparison of techniques for finding coefficients of polynomial chaos models for antenna problems. *Int. J. RF Microw. Comput. Aided. Eng.* **2021**, *31*, e22729. [[CrossRef](#)]
33. Boeykens, F.; Rogier, H.; Vallozzi, L. An efficient technique based on polynomial chaos to model the uncertainty in the resonance frequency of textile antennas due to bending. *IEEE Trans. Ant. Prop.* **2014**, *62*, 1253–1260. [[CrossRef](#)]
34. Yu, Z.; Sun, Z.; Cao, R.; Wang, J.; Yan, Y. RCA-PCK: A new structural reliability analysis method based on PC-Kriging and radial centralized adaptive sampling strategy. *Proc. Inst. Mech. Eng. Part C J. Mech. Eng. Sci.* **2021**, *235*, 3424–3438. [[CrossRef](#)]
35. Schobi, R.; Sudret, B.; Wiart, J. Polynomial-chaos-based kriging. *Int. J. Uncertain. Quantif.* **2015**, *5*, 171–193. [[CrossRef](#)]
36. Ochoa, J.S.; Cangellaris, A.C. Random-space dimensionality reduction for expedient yield estimation of passive microwave structures. *IEEE Trans. Microw. Theory Tech.* **2013**, *61*, 4313–4321. [[CrossRef](#)]
37. Rayas-Sanchez, J.E.; Gutierrez-Ayala, V. EM-based Monte Carlo analysis and yield prediction of microwave circuits using linear-input neural-output space mapping. *IEEE Trans. Microw. Theory Tech.* **2006**, *54*, 4528–4537. [[CrossRef](#)]
38. Zhang, J.; Feng, F.; Na, W.; Yan, S.; Zhang, Q. Parallel space-mapping based yield-driven EM optimization incorporating trust region algorithm and polynomial chaos expansion. *IEEE Access* **2019**, *7*, 143673–143683. [[CrossRef](#)]
39. Zhang, C.; Na, W.; Zhang, Q.J.; Bandler, J.W. Fast yield estimation and optimization of microwave filters using a cognition-driven formulation of space mapping. In Proceedings of the 2016 IEEE MTT-S International Microwave Symposium (IMS), San Francisco, CA, USA, 22–27 May 2016; pp. 1–4.
40. Hassan, A.-K.S.; Mohamed, A.S.; El-Sharabasy, A.Y. EM-based yield optimization exploiting trust-region optimization and space mapping technology. *Int. J. RF Microw. Comp. Aid. Eng.* **2015**, *25*, 474–484. [[CrossRef](#)]
41. Kennedy, M.C.; O'Hagan, A. Predicting the output from complex computer code when fast approximations are available. *Biometrika* **2000**, *87*, 1–13. [[CrossRef](#)]
42. Lefebvre, J.-P.; Dompierre, B.; Robert, A.; Le Bihan, M.; Wyart, E.; Sainvitu, C. Failure probability assessment using co-kriging surrogate models. *Procedia Eng.* **2015**, *133*, 622–630. [[CrossRef](#)]

43. Spina, D.; Ferranti, F.; Antonini, G.; Dhaene, T.; Knockaert, L. Efficient variability analysis of electromagnetic systems via polynomial chaos and model order reduction. *IEEE Trans. Comp. Packag. Manuf. Tech.* **2014**, *4*, 1038–1051. [[CrossRef](#)]
44. Kouassi, A.; Nguyen-Trong, N.; Kaufmann, T.; Lallechere, S.; Bonnet, P.; Fumeaux, C. Reliability-aware optimization of a wideband antenna. *IEEE Trans. Ant. Prop.* **2016**, *64*, 450–460. [[CrossRef](#)]
45. Scotti, G.; Tommasino, P.; Trifiletti, A. MMIC yield optimization by design centering and off-chip controllers. *IET Proc.-Circuits Devices Syst.* **2005**, *152*, 54–60. [[CrossRef](#)]
46. Zhang, J.; Feng, F.; Jin, J.; Zhang, W.; Zhao, Z.; Zhang, Q.J. Adaptively weighted yield-driven EM optimization incorporating neurotransfer function surrogate with applications to microwave filters. *IEEE Trans. Microw. Theory Tech.* **2021**, *69*, 518–528. [[CrossRef](#)]
47. Zhang, J.; Na, W.; Feng, F. Yield-driven EM optimization exploiting parallel computation and EM sensitivities. In Proceedings of the 2020 13th UK-Europe-China Workshop on Millimetre-Waves and Terahertz Technologies (UCMMT), Tianjin, China, 29 August–1 September 2020; pp. 1–3.
48. Abdel-Malek, H.L.; Hassan, A.S.O.; Soliman, E.A.; Dakroury, S.A. The ellipsoidal technique for design centering of microwave circuits exploiting space-mapping interpolating surrogates. *IEEE Trans. Microw. Theory Tech.* **2006**, *54*, 3731–3738. [[CrossRef](#)]
49. Rayas-Sanchez, J.E.; Gutierrez-Ayala, V. EM-based statistical analysis and yield estimation using linear-input and neural-output space mapping. In Proceedings of the 2006 IEEE MTT-S International Microwave Symposium Digest, San Francisco, CA, USA, 11–16 June 2006; pp. 1597–1600.
50. Zhang, J.; Zhang, C.; Feng, F.; Zhang, W.; Ma, J.; Zhang, Q.J. Polynomial chaos-based approach to yield-driven EM optimization. *IEEE Trans. Microw. Theory Tech.* **2018**, *66*, 3186–3199. [[CrossRef](#)]
51. Koziel, S.; Bekasiewicz, A. Sequential approximate optimization for statistical analysis and yield optimization of circularly polarized antennas. *IET Microw. Ant. Prop.* **2018**, *12*, 2060–2064. [[CrossRef](#)]
52. Koziel, S.; Bandler, J.W. Rapid yield estimation and optimization of microwave structures exploiting feature-based statistical analysis. *IEEE Trans. Microw. Theory Tech.* **2015**, *63*, 107–114. [[CrossRef](#)]
53. Koziel, S.; Bekasiewicz, A. Reduced-cost surrogate modeling of input characteristics and design optimization of dual-band antennas using response features. *Int. J. RF Microw. CAE* **2018**, *28*, e21194. [[CrossRef](#)]
54. Koziel, S. Low-cost data-driven surrogate modeling of antenna structures by constrained sampling. *IEEE Antennas Wirel. Prop. Lett.* **2017**, *16*, 461–464. [[CrossRef](#)]
55. Koziel, S.; Pietrenko-Dabrowska, A. Performance-based nested surrogate modeling of antenna input characteristics. *IEEE Trans. Ant. Prop.* **2019**, *67*, 2904–2912. [[CrossRef](#)]
56. Koziel, S.; Pietrenko-Dabrowska, A. Reduced-cost surrogate modelling of compact microwave components by two-level kriging interpolation. *Eng. Optim.* **2020**, *52*, 960–972. [[CrossRef](#)]
57. Koziel, S.; Pietrenko-Dabrowska, A. Reliable data-driven modeling of high-frequency structures by means of nested kriging with enhanced design of experiments. *Eng. Comp.* **2019**, *36*, 2293–2308. [[CrossRef](#)]
58. Koziel, S.; Pietrenko-Dabrowska, A. Low-cost performance-driven modelling of compact microwave components with two-layer surrogates and gradient kriging. *AEU-Int. J. Electron. Commun.* **2020**, *126*, 153419. [[CrossRef](#)]
59. Pietrenko-Dabrowska, A.; Koziel, S. Surrogate modeling of impedance matching transformers by means of variable-fidelity EM simulations and nested co-kriging. *Int. J. RF Microw. Comput. Aided Eng.* **2020**, *30*, e22268. [[CrossRef](#)]
60. Koziel, S.; Bekasiewicz, A. Low-cost surrogate-assisted statistical analysis of miniaturized microstrip couplers. *J. Electromagn. Waves Appl.* **2016**, *30*, 1345–1353. [[CrossRef](#)]
61. Simpson, T.W.; Pelplinski, J.D.; Koch, P.N.; Allen, J.K. Metamodels for computer-based engineering design: Survey and recommendations. *Eng. Comput.* **2001**, *17*, 129–150. [[CrossRef](#)]
62. Queipo, N.V.; Haftka, R.T.; Shyy, W.; Goel, T.; Vaidynathan, R.; Tucker, P.K. Surrogate based analysis and optimization. *Prog. Aerosp. Sci.* **2005**, *41*, 1–28. [[CrossRef](#)]
63. Pietrenko-Dabrowska, A.; Koziel, S.; Al-Hasan, M. Expedited yield optimization of narrow- and multi-band antennas using performance-driven surrogates. *IEEE Access* **2020**, *8*, 143104–143113. [[CrossRef](#)]
64. Conn, A.R.; Gould, N.I.M.; Toint, P.L. *Trust Region Methods*; MPS-SIAM: Philadelphia, PA, USA, 2000.
65. Broyden, C.G. A class of methods for solving nonlinear simultaneous equations. *Math. Comp.* **1965**, *19*, 577–593. [[CrossRef](#)]
66. Pietrenko-Dabrowska, A. Rapid tolerance-aware design of miniaturized microwave passives by means of confined-domain surrogates. *Int. J. Numer. Model.* **2020**, *33*, e2779. [[CrossRef](#)]
67. Koziel, S.; Bekasiewicz, A. On reduced-cost design-oriented constrained surrogate modeling of antenna structures. *IEEE Ant. Wirel. Prop. Lett.* **2017**, *16*, 1618–1621. [[CrossRef](#)]
68. Koziel, S.; Bekasiewicz, A.; Kurgan, P.; Bandler, J.W. Expedited multi-objective design optimization of miniaturized microwave structures using physics-based surrogates. In Proceedings of the 2015 IEEE MTT-S International Microwave Symposium, Phoenix, AZ, USA, 17–22 May 2015; pp. 1–3.